Anomalous Hall effect due to spin chirality in the Kagomé lattice

M. Taillefumier,[1,2] B. Canals,[1] C. Lacroix,[1] V. K. Dugaev,[1,2,3] and P. Bruno[2]
[1]*Laboratoire Louis Néel, CNRS, 25 avenue des martyrs, Boîte Postale 166, 38042 Grenoble Cedex 09, France*
[2]*Max-Planck-Institut für Mikrostrukturphysik, Weinberg 2, D-06120 Halle, Germany*
[3]*Department of Physics and CFIF, Instituto Superior Técnico, Avenida Rovisco Pais, 1049-001 Lisbon, Portugal*
(Received 26 January 2006; published 2 August 2006)

We consider a model for a two-dimensional electron gas moving on a Kagomé lattice and locally coupled to a chiral magnetic texture. We show that the transverse conductivity σ_{xy} does not vanish even if spin-orbit coupling is not present and it may exhibit unusual behavior. The model parameters are the chirality, the number of conduction electrons, and the amplitude of the local coupling. Upon varying these parameters, a topological transition characterized by change of the band Chern numbers occurs. As a consequence, σ_{xy} can be quantized, proportional to the chirality, or have a nonmonotonic behavior upon varying these parameters.

DOI: 10.1103/PhysRevB.74.085105 PACS number(s): 72.15.−v, 71.10.Fd, 75.10.Lp

I. INTRODUCTION

In ferromagnetic systems, there are two contributions to the transverse resistivity ρ_{xy}: one is due to the usual Lorentz force acting on the electrons when a magnetic field is applied, R_0B, and the second one, R_sM, is proportional to the magnetization of the ferromagnet. This is called the anomalous Hall effect.

The origin of this anomalous Hall effect (AHE) has long been controversial and both extrinsic (impurities) and intrinsic mechanisms have been discussed. Karplus and Luttinger[1] proposed that this effect is a consequence of spin-orbit interaction in metallic ferromagnets. Then it was argued that impurities give the main contribution to the anomalous Hall effect and usually two mechanisms, both due to spin-orbit coupling, contribute. One is known as the side-jump mechanism[2,3] and it predicts that the Hall resistivity R_s is proportional to the longitudinal resistivity ρ. The second one[4,5] is the skew-scattering mechanism, which gives a contribution proportional to ρ^2.

In recent years several groups have measured an anomalous Hall effect in various systems which cannot be attributed to the usual mechanisms (skew scattering or side jump). A new intrinsic mechanism, related to the noncollinear spin configuration, with a ferromagnetic component, was first proposed for manganites:[6–8] in these systems deviation from collinearity is a consequence of the competition between double exchange, superexchange, and spin-orbit interactions. Then it was proposed that a similar mechanism works in spin-glass systems where the spin configuration is highly noncoplanar:[9,10] in the weak-coupling limit it was shown that the Hall resistivity is proportional to a uniform chirality parameter with a sign that depends on the details of the band structure. This chirality parameter was defined by Tatara and Kawamura[9] for three spins at sites i,j,k as a scalar quantity $\chi=\langle \mathbf{S}_i\cdot(\mathbf{S}_j\times\mathbf{S}_k)\rangle$, which is nonzero if the spins are noncoplanar. Very recently several groups confirmed the existence of such a contribution in typical AuFe spin glasses.[11,12]

In nondisordered systems, the same mechanism can work if the ordered magnetic structure is noncoplanar. This is realized in several pyrochlore compounds such as $Nd_2Mo_2O_7$ for which Taguchi *et al.*[13] proposed that an anomalous contribution to the Hall effect is related to the umbrella structure of both Nd and Mo moments in the long-range-ordered phase. Detailed studies of this system and other pyrochlores ($Sm_xY_{1-x}Mo_2O_7$, $Nd_xY_{1-x}Mo_2O_7$) have been performed,[13–15] leading to some controversy: using neutron diffraction experiments in a magnetic field it is possible to calculate the T and H dependence of both the Mo and Nd chiral order parameters and in Ref. 15 it was concluded that the chiral mechanism alone cannot explain the T dependence of the Hall coefficient in pyrochlores.

From the theoretical point of view, this mechanism is often called the "Berry phase contribution" because a nonvanishing spin chirality is associated with a nonvanishing Berry phase for conduction electrons coupled via local Hund's exchange interaction to the spins. Ohgushi *et al.*[16] calculated the Hall effect in a Kagomé lattice with a noncoplanar long-range spin structure. They showed that, in the adiabatic limit, when the electron conduction spins are aligned with localized spins at each site of the lattice (this corresponds to infinite Hund's coupling), the Berry phase contribution to the Hall conductivity is quantized for some values of the band filling. In this paper, we study a model that extrapolates between this strong-coupling limit and the weak-coupling case studied by Tatara and Kawamura.[9] We show also that the Berry phase contribution depends not only on the chirality, but also on the strength of the local Hund's coupling and on the band filling.

II. MODEL

A. Hamiltonian

The aim of this work is to show how the transport properties of electrons are influenced by two different contributions. First, the electrons are restricted to move on a lattice and are therefore experiencing its geometry. This results in a peculiar band structure. Second, each electron has its spin

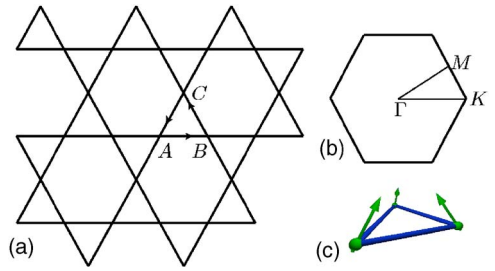

FIG. 1. (Color online) (a) The Kagomé lattice is described as a triangular lattice of triangles. Its Bravais vectors are $a_1=(1,0)$, $a_2=(-1/2,\sqrt{3}/2)$, and $a_3=-(1/2,\sqrt{3}/2)$, connecting, respectively, the points A to B, B to C, and C to A. (b) The first Brillouin zone is a hexagon with the corners located at $k=\pm(2\pi/3)a_1$, $k=\pm(2\pi/3)a_2$, and $k=\pm(2\pi/3)a_3$. (c) The umbrella structure on the triangular cell of the Kagomé lattice.

locally coupled to a given distribution of magnetic moments on each site of the lattice.

Both effects are taken into account in the following Hamiltonian:

$$\mathcal{H}=\sum_{\langle i,j\rangle,\sigma} t_{ij}(c_{i\sigma}^{\dagger}c_{j\sigma}+\text{H.c.})-J\sum_{i} c_{i\alpha}^{\dagger}(\boldsymbol{\sigma}_{\alpha\beta}\cdot\mathbf{S}_i)c_{i\beta}. \quad (1)$$

The first term describes the electrons moving on the lattice: t_{ij} is the hopping integral between two neighboring sites i and j; $c_{i\sigma}^{\dagger}$ and $c_{i\sigma}$ are the creation and annihilation operators of an electron with spin σ on the site i. The second part of the Hamiltonian couples the electron spin to a local moment on each site.

The coupling constant to each local moment $\mathbf{S}_i$ is J, and these moments are treated below as classical variables. $\boldsymbol{\sigma}_{\alpha\beta}$ are the Pauli matrices. The underlying lattice is the Kagomé lattice, depicted in Fig. 1. It is a two-dimensional tiling of corner-sharing triangles, described as a triangular lattice of triangles throughout this paper.

This Hamiltonian has already been discussed in the limit of $J\to\infty$ by Ohgushi *et al.*[16] In this limit the two $\sigma=\uparrow,\downarrow$ bands are infinitely split and the model describes a fully polarized electron gas subject to a modulation of a fictitious magnetic field, corresponding to the molecular field associated with the magnetic texture. The comparison with the present work will be done later on. In the general case of finite J, the calculations must be done numerically. It is worth noting that the sign of J is unimportant in this classical treatment since changing J to $-J$ is equivalent to an exchange of $\uparrow$ and $\downarrow$ spin states.

B. Parameters and motivation

We consider the spin texture as a "parameter" of the model. The local moments $\mathbf{S}_i$ are described classically, and the chosen magnetic phase is periodic, thus allowing us to work in the reciprocal space. The choice of the magnetic arrangement is motivated by two facts. First, we are interested in describing anomalous transport properties of the type already addressed in previous works (see Refs. 14, 16, and 17) in which it has been argued that the transverse conductivity may be related to the chirality of the magnetic phase. Second, an unusual mechanism of the AHE has recently been proposed, based on an unconventional chiral magnetic ordering due to geometrical frustration,[14,18–20] but with controversial interpretations. We therefore consider the present model as a simple model to address these problems, and clearly identify each relevant contribution.

We consider a magnetic phase that has been obtained by studying a pure spin model with anisotropic Dzyaloshinskii-Moriya interactions on a Kagomé lattice.[21] It consists of an umbrella of three spins per unit cell of the Kagomé lattice (see Fig. 1). Each umbrella can be described by the spherical coordinates of the three spins $(\pi/6,\theta)$, $(5\pi/6,\theta)$, and $(-\pi/2,\theta)$. The angle θ ranges from 0 (all the spins are perpendicular to plane, and the corresponding ordering is ferromagnetic) to π. It is worth noting that the usual three-sublattice planar magnetic phase belonging to the ground-state manifold of the Kagomé antiferromagnet, commonly denoted as the "$q=0$ phase," corresponds to $\theta=\pi/2$.

In between, all phases are possible and chiral, where the chirality is defined as the mixed product of three spins on a plaquette,

$$\chi_{ijk}=\mathbf{S}_i\cdot(\mathbf{S}_j\times\mathbf{S}_k)=\frac{3\sqrt{3}}{2}\cos\theta\sin^2\theta. \quad (2)$$

All these phases ($\theta\in[0,\pi]$) are therefore translation invariant but do not have time-reversal symmetry.

We consider the local spins as classical spins with length M and we introduce in Eq. (1) an effective coupling constant $J_0=JM$ which allows us to rewrite the Hamiltonian as

$$\mathcal{H}=\sum_{\langle i,j\rangle,\sigma} t_{ij}(c_{i\sigma}^{\dagger}c_{j\sigma}+\text{H.c.})-J_0\sum_{i} c_{i\alpha}^{\dagger}(\boldsymbol{\sigma}_{\alpha\beta}\cdot\mathbf{n}_i)c_{i\beta} \quad (3)$$

where $\mathbf{n}_i$ is a unit vector collinear with the local moment $\mathbf{S}_i$.

Setting $t=|t_{ij}|$ as the energy unit, our free parameters are the angle θ, parametrizing the chirality of the magnetic texture, and the value of J_0. The Fermi level, through the filling factor p of the bands, can also be varied. Each of these variables gives a different contribution as will be discussed in the next sections.

C. Physical quantities

Before calculating any physical observables, we have to diagonalize the Hamiltonian of Eq. (1). For this purpose, the Hamiltonian is rewritten in the reciprocal space as

$$\mathcal{H}=\sum_{\mathbf{k}}\Psi_{\mathbf{k}}^{\dagger}h_{\mathbf{k}}\Psi_{\mathbf{k}}+\text{H.c.}, \quad (4)$$

where $\Psi_{\mathbf{k}}=(c_{A\mathbf{k}\uparrow},c_{B\mathbf{k}\uparrow},c_{C\mathbf{k}\uparrow},c_{A\mathbf{k}\downarrow},c_{B\mathbf{k}\downarrow},c_{C\mathbf{k}\downarrow})$, A, B, and C are the corners of the Kagomé lattice unit cell [Fig. 1(a)],

$$c_{A\mathbf{k}\sigma}=\sum_{j} c_{A,j,\sigma}e^{i\mathbf{k}\cdot\mathbf{r}_{ij}}, \quad (5)$$

is the Fourier transform of $c_{A,j,\sigma}$, and $r_{Aj}=r_A+R_j$ with R_j the lattice vector and r_A the position of the moment $\mathbf{S}_A$ in the unit cell. $h_{\mathbf{k}}$ is a 6×6 matrix given by

$$h_{\mathbf{k}} = \begin{pmatrix} -J_0\cos\theta & p_k^1 & p_k^3 & -J_0\sin\theta e^{i\pi/6} & 0 & 0 \\ p_k^1 & -J_0\cos\theta & p_k^2 & 0 & -J_0\sin\theta e^{i5\pi/6} & 0 \\ p_k^3 & p_k^2 & -J_0\cos\theta & 0 & 0 & iJ_0\sin\theta \\ -J_0\sin\theta e^{-i\pi/6} & 0 & 0 & J_0\cos\theta & p_k^1 & p_k^3 \\ 0 & -J_0\sin\theta e^{-i5\pi/6} & 0 & p_k^1 & J_0\cos\theta & p_k^2 \\ 0 & 0 & -iJ_0\sin\theta & p_k^3 & p_k^2 & J_0\cos\theta \end{pmatrix}, \tag{6}$$

with $t=|t_{ij}|$ and $p_{\mathbf{k}}^i=2t\cos(\mathbf{k}\cdot\mathbf{a}_i)$.

To calculate the anomalous Hall effect, we use the expression of the off-diagonal conductivity using the following Kubo formula in the limit of a disorder-free electron gas:[22]

$$\sigma_{xy}(\omega) = \frac{e^2\hbar}{S}\sum_{n\neq m}\sum_{\mathbf{k}}(f_{n\mathbf{k}}-f_{m\mathbf{k}}) \times \frac{\langle n,\mathbf{k}|v_x|m,\mathbf{k}\rangle\langle n,\mathbf{k}|v_y|m,\mathbf{k}\rangle}{(\varepsilon_{n\mathbf{k}}-\varepsilon_{m\mathbf{k}})(\varepsilon_{n\mathbf{k}}-\varepsilon_{m\mathbf{k}}-\omega)}, \tag{7}$$

where S is the surface of the unit cell, and $\varepsilon_{n\mathbf{k}}$ is the eigenvalue of matrix (6) corresponding to the energy of the nth band for the wave vector $\mathbf{k}$, with the eigenvector $|n,\mathbf{k}\rangle$. Here $v_i=\frac{1}{\hbar}\frac{\partial h_{\mathbf{k}}}{\partial k_i}$ is the velocity of electrons $(i=x,y,z)$. Taking the static limit of $\omega\to 0$, Eq. (7) becomes

$$\sigma_{xy} = \frac{e^2\hbar}{S}\sum_{n,\mathbf{k}} f_{n,\mathbf{k}}\sum_{m\neq n}\frac{(v_x)^{nm}(v_y)^{mn}-(v_x)^{mn}(v_y)^{nm}}{(\varepsilon_{n,\mathbf{k}}-\varepsilon_{m,\mathbf{k}})^2} = \frac{e^2}{\hbar S}\sum_{n,\mathbf{k}} f_{n,\mathbf{k}}[\boldsymbol{\nabla}_{\mathbf{k}}\times\mathbf{A}_{n\mathbf{k}}]_z, \tag{8}$$

where $\mathbf{A}_{n\mathbf{k}}=-i\langle n\mathbf{k}|\boldsymbol{\nabla}_{\mathbf{k}}|n\mathbf{k}\rangle$ is the geometric vector potential and $f_{n\mathbf{k}}$ is the Fermi-Dirac distribution function.

The expression (8) is similar to that obtained by Thouless *et al.*[23] in the context of the quantized Hall effect in two dimensions. In particular, when the band is completely filled, the circulation of $\mathbf{A}_{n\mathbf{k}}$ or the flux of the Berry curvature defined as $\boldsymbol{\Omega}_{n\mathbf{k}}=\boldsymbol{\nabla}_{\mathbf{k}}\times\mathbf{A}_{n\mathbf{k}}$ over the first Brillouin zone is equal to 2π times an integer[23,24] called the Chern number ν_n. Expression (8) of the off-diagonal conductivity finally becomes

$$\sigma_{xy} = \frac{e^2}{\hbar S}\sum_{n\mathbf{k}} f_{n\mathbf{k}}\Omega_{n\mathbf{k}}^z = \frac{e^2}{h}\sum_n \nu_n, \tag{9}$$

where $\nu_n=\frac{1}{2\pi}\int f_{n\mathbf{k}}\Omega_{n\mathbf{k}}^z d^2\mathbf{k}$. As we shall see, this implies that the Hall conductivity is quantized when the Fermi level lies in a gap.

The Chern numbers have the following properties: (i) the sum over all bands is equal to 0; (ii) if, for some peculiar values of parameters of the model, the energy bands m and n cross each other at some point of the Brillouin zone, their respective Chern numbers obey the conservation rule

$$(\nu_m+\nu_n)_b = (\nu_m+\nu_n)_a \tag{10}$$

where the indices b,a refer to the values of the Chern number before and after the bands are touching each other.[25] We will check each of these conservation rules in the next sections.

It should be noticed that the sum over $\mathbf{k}$ in Eq. (9) runs over all occupied states. This may seem unusual as in metallic systems we expect that only the quasiparticles near the Fermi surface contribute to transport properties. However, it has been recently shown by Haldane[26] that Eq. (9) can be reconciled with this point of view and reduced to a sum over the states near the Fermi energy.

III. NUMERICAL RESULTS

This section is divided in two parts. In the first one, the band structure is calculated for different angles θ and coupling constants J_0. The evidence for two different regimes of coupling is given, illustrated by the variation of the Chern numbers. In the second one, we focus on the transverse conductivity at zero temperature. It is shown that the chirality may be a relevant quantity for describing the transverse conductivity $(\sigma\propto\chi)$ in some ranges of coupling only for a half-filled band.

A. Band structure and associated Chern numbers

The energy spectrum of the Kagomé lattice in the absence of exchange interaction is characterized by one flat band at $E=2t$ and two dispersive bands, which touch each other at the $\mathbf{k}$ point K of the Brillouin zone as shown in Fig. 2. This peculiarity has already been addressed in the context of spin models as well as for metallic systems.[27]

When the coupling constant J_0 is nonzero, the energy spectrum splits into two parts due to the spin-dependent potential. For very large values of J_0, the spectrum is divided into two groups of three bands, which is the case studied by Ohgushi *et al.*[16] In between, for nonzero but not too large values of J_0, the spectrum can only be computed numerically, except for the special cases of $\theta=0$ or π, or for general θ at high-symmetry points. For these intermediate values of J_0, the splitting of the spectrum depends qualitatively on two mechanisms.

First, the coupling J_0 gradually separates each group of three bands taking them from degenerate for $J_0=0$ to fully separated for infinite J_0. Second, within each group of three bands, pointlike degeneracies are lifted (see Fig. 2, points Γ and K) when switching on J_0, and finally restored for $J_0\to\infty$ (see Ref. 16). The numerical calculation of the spectrum

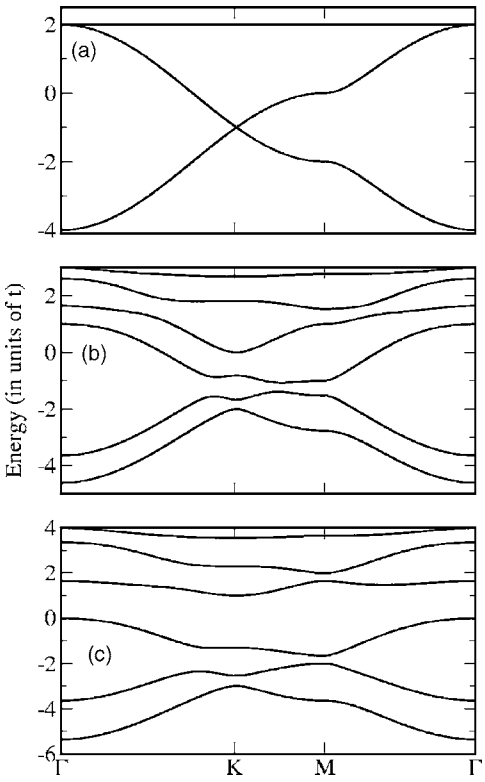

FIG. 2. (a) Energy spectrum of Eq. (14) calculated for $J_0=0$. Each band is twice degenerate due to the spin degeneracy. (b) Energy spectrum calculated for $J_0=t$ and $\theta=\pi/3$. (c) Energy spectrum calculated for $J_0=2t$ and $\theta=\pi/3$. The critical value J_c is equal to $4t/\sqrt{7}\approx 1.51t$.

shows that it is either gapless for small values of J_0, or has gaps for higher values.

When a gap opens, it always occurs at the M point of the Brillouin zone. This allows us to compute analytically the critical value of the coupling as a function of chirality parametrized by the angle θ,

$$J_c(\theta) = \pm \frac{2t}{\sqrt{1+3\cos^2\theta}}. \tag{11}$$

Using Eq. (11) we can distinguish between two different regimes (Fig. 2) depending on the value of J_0 as compare to $J_c(\theta)$. These regimes are characterized by a particular organization of the band structure as shown in Figs. 2(b) for $J_0=t$ and 2(c) for $J_0=2t$ and different Chern numbers. For $J_0>J_c(\theta)$, the Chern numbers associated with each band are given by −1, 0, 1, 1, 0, −1 from the lowest to the topmost band. Those numbers were obtained by Ohgushi *et al.*[16] in the limit of $J_0\to\infty$. When $J_0<J_c$, the Chern numbers associated with this configuration are −1, 3, −2, −2, 3, −1 given in the same order as in the previous case. The global sum rule $\Sigma_n \nu_n=0$ is always verified as well as the local one around the critical coupling where two pairs of bands are crossing each other. It reads as

$$\nu_2+\nu_3=1 \quad \text{and} \quad \nu_4+\nu_5=1 \tag{12}$$

below and above the critical coupling J_c, respectively. The corresponding phase diagram is shown in Fig. 3.

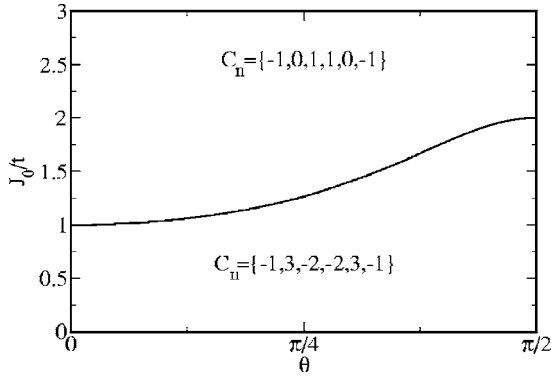

FIG. 3. The phase diagram in J_0-θ variables. The black line is given by Eq. (11) and corresponds to the vanishing gap between bands 2 and 3 (the gap between bands 4 and 5 also vanishes).

B. Off-diagonal conductivity at $T=0$

The off-diagonal conductivity is computed using Eq. (7) at $T=0$ for different values of the chirality θ and the amplitude of the exchange interaction J_0.

As shown in Fig. 4 [the corresponding energy spectrum is presented in Figs. 2(b) and 2(c)] at $T=0$, the Hall conductivity is quantized when the Fermi level lies in the gap. The value of the plateau depends explicitly on the Chern number of the filled bands. When the Fermi level is in a band, the sum (9) can be reformulated in terms of a sum over the Fermi level as shown by Haldane[26] recently. One has to note that when the Fermi level and θ are fixed, any variation of J_0 around $J_c(\theta)$ may induce a jump in the Hall conductivity. For instance, with a filling factor $p=1/3$ [Fig. 5(a)], the Fermi level always lies in a gap but the off-diagonal conductivity jumps from $-e^2/h$ for $J_0>J_c$ to $2e^2/h$ for $J_0<J_c$.

A similar jump can be obtained if θ is changed, while J_0 is constant: such a change in θ can, for example, be induced by

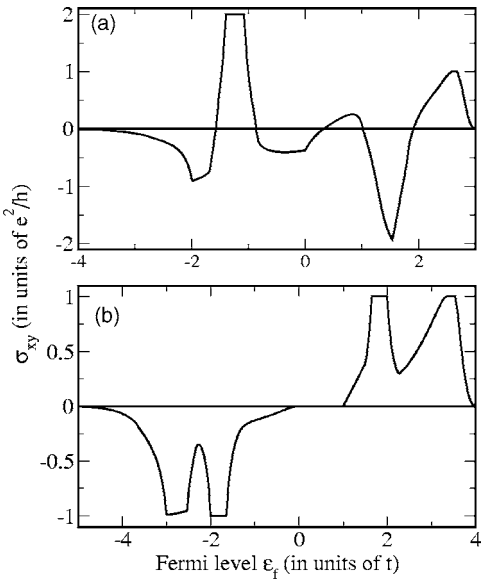

FIG. 4. Off-diagonal conductivity evaluated at $T=0$ as a function of ε_f for $\theta=\pi/3$ and $J_0=t$ (a) and (b) $2t$. In both cases, σ_{xy} is quantized when the Fermi level lies in a gap. The values of the plateaus depend strongly on the topology of the energy spectrum.

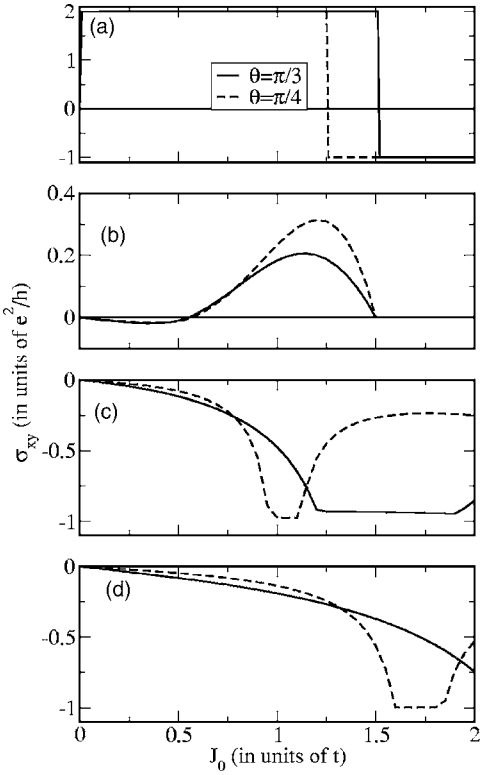

FIG. 5. Off-diagonal conductivity $\sigma_{xy}(J)$ evaluated at $T=0$ for a filling factor $p=1/3$ (a), $1/2$ (b), $1/4$ (c), and $1/5$ (d); and $\theta=\pi/3$ (continuous lines) and $\pi/4$ (dashed lines).

application of an external magnetic field perpendicular to the Kagomé plane. In this case, a large change of the Hall conductivity (even a sign change) can be induced by a magnetic field.

This is not the case for $p=1/2$. For that filling factor, the Hall conductivity varies smoothly when J_0 passes through the point $J_0=3t/2$, which does not depend on θ [Fig. 5(b)]. When $J_0<3t/2$, the Fermi level crosses bands 3 and 4, resulting in a nonzero Hall conductivity. When $J_0>3t/2$, the Fermi level is in the gap separating bands 3 and 4 and the off-diagonal conductivity is given by the sum of the Chern numbers of the first three bands, which gives zero.

Figure 5 shows the variation of the Hall conductivity as a function of J_0 for filling factors $1/4$ [Fig. 5(c)] and $1/5$ [Fig. 5(d)]: in both cases the Fermi level is not in a gap and the Hall conductivity does not exhibit any jump.

From these comments, it is clear that the chirality is never a relevant parameter for the Hall conductivity when the Fermi level lies in a gap, because σ_{xy} is then quantized and, obviously, not proportional to the chirality.

Conversely, it is possible to choose a filling factor such that the Fermi level is not within a gap. In Fig. 6, we present σ_{xy} versus θ for the filling factor $p=1/2$ (a) and (b) and different values of J_0. For this filling factor, the Fermi level is not in a gap if $J_0<3t/2$. Scaling the conductivity by its maximal value in each case shows that it is proportional to chirality in a large range of coupling J_0, whatever the value of the chirality. This is somewhat unexpected as the previous studies relating σ_{xy} to χ were restricted to small values of J_0.[9] However, for different values of the band filling this is

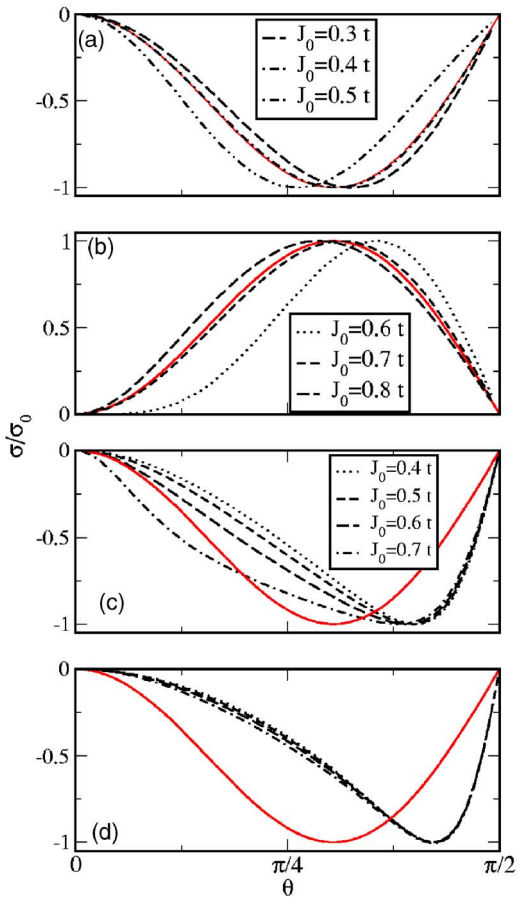

FIG. 6. (Color online) σ_{xy}/σ_0 with $\sigma_0=\max(|\sigma_{xy}|)$ versus angle θ, calculated for a filling factor $p=1/2$ (a) and (b), $1/4$ (c), and $1/5$ (d), and different values of J_0. The continuous line represents the chirality given by Eq. (2). The Hall conductivity is represented by the dashed lines for different values of the parameter J_0. We remark that σ_{xy} changes sign when J_0 tends to $0.6t$. That change is related to the position of the Fermi level within the band but not associated with change of the Chern numbers. It is remarkable that the conductivity is more or less proportional to the chirality in a large range of couplings, up to $J_0\approx t$, as well as for large χ values. For $p=1/4$ and $1/5$, one can show that the off-diagonal conductivity is not proportional to the chirality even for small values of J_0.

no longer true as shown on Fig. 6 for $p=1/4$ [Fig. 6(c)] and $1/5$ [Fig. 6(d)]: for these filling factors, σ_{xy} is sensitive to the variation of the Chern numbers when J_0 varies. In fact we found that the Hall conductivity is proportional to chirality only for $p=1/2$ and small enough J_0.

IV. DISCUSSION

The model studied in this paper cannot be directly applied to materials in which the anomalous Hall effect attributed to spin chirality has been observed.

However, some interesting features have been obtained in this model. This work shows that the transverse conductivity may be proportional to chirality in the strong-coupling regime, extending previous results obtained in the weak-coupling case[9] but this occurs only for a half-filled band. It is

also shown that the dependence of σ_{xy} not only is determined by the chirality but also depends strongly on the exchange coupling parameter and on the band filling factor. σ_{xy} can present a large variety of behaviors: nonmonotonic variation, sign change, or plateaus can be observed. Thus, even if the underlying magnetic phase chirality is the main origin of this intrinsic anomalous Hall effect, it is far from being entirely determined by the chirality.

We suggest that in real systems, variation of the coupling J can be induced by temperature: the temperature acts on the system in many different ways. It acts on the magnetic configuration of the localized spins $\mathbf{S}_i$ by changing the amplitude of the magnetization, and on the position of the Fermi level in the band through the Fermi-Dirac distribution.

We assume that the magnitude of each local moment follows the mean field relation

$$M(T) = |\mathbf{S}_i| = M_0 \sqrt{1 - \frac{T}{T_c}}, \tag{13}$$

where T_c is the critical temperature. This can be described by introducing in Eq. (1) a temperature-dependent coupling constant

$$J(T) = J_0 \sqrt{1 - \frac{T}{T_c}}, \tag{14}$$

where $J_0 = JM_0$ is the zero-temperature exchange constant and J_0 and T_c are supposed to be independent.

Consequently, decreasing the temperature from T_c to $T=0$ is equivalent to increasing the exchange coupling from $J=0$ to J_0. This increase of J can be considered as done at zero temperature since in a large range of parameters, the additional effect of temperature [i.e., the T dependance of the Fermi function in Eq. (8)], is significant only when the Fermi level is very close to a band edge.

Qualitatively, this means that when the temperature is decreased, one moves vertically from the bottom to the top of the phase diagram in Fig. 3: if J_0 is large enough, the temperature decrease produces, at some particular temperature $T_\star$ such that $J(T_\star) = J_c(T=0)$, a change in conductivity due to the change of the Chern numbers. From this observation it follows that σ_{xy} can show abrupt changes with temperature. It is worth noting that during that process, in the frame of our model, the magnetic texture characterized by its θ angle has *not* moved. Of course, a change in θ can also be responsible for a sign change.

To be more specific, we consider several examples presented in Fig. 7.

We start with the filling factor $p=1/2$, the critical temperature $T_c = 0.1t$, and $J(T=0) = 2t$ [Fig. 7(a)]. With this choice of parameters, the Fermi level lies in a gap when $J_0 > 3t/2$, which means that at low temperatures (i.e., for large J_0), the system is insulating. When the temperature is increased, σ_{xy} remains equal to zero untill T reaches the temperature T_1 for which $J(T_1) = 3t/2$. Above this temperature, the gap closes, making the transverse conductivity increase continuously. It reaches an extremum which is a function of the texture angle θ. Just below T_c, σ_{xy} changes sign because of a subtle balance between the states giving positive and negative contributions to the conductivity, namely, the states from bands 3 and 4 (negative contribution) and the states from band 2 (positive contribution). These contributions may be globally explained by the associated Chern numbers of these bands, at small J_0, ν_3, $\nu_4 = -2$ and $\nu_2 = 3$.

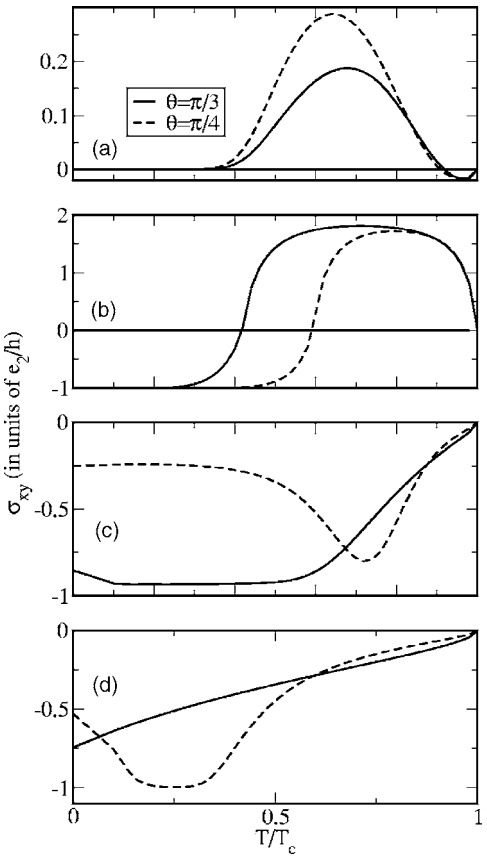

FIG. 7. Off-diagonal conductivity $\sigma_{xy}(T)$ for a filling factor $p=1/2$ (a), $1/3$ (b), $1/4$ (c), and $1/5$ (d); and $\theta = \pi/3$ (continuous lines) and $\pi/4$ (dashed lines).

For the filling factor $p=1/3$ [Fig. 7(b)], the behavior is completely different. The transverse conductivity is quantized and finite at zero temperature as the Fermi level is located in a gap. When the temperature increases and reaches the value $T_\star$ defined by $J(T_\star) = J_c(\theta)$, for which gaps are finite but sufficiently small to allow interband processes, σ_{xy} continuously increases. Upon increasing temperature, the conductivity increases and then changes its sign. This change of sign is not of the same origin as we considered for $p=1/2$. In the first case, the Chern numbers are fixed but the temperature changes the balance between the weights of each band. In the second example, bands 3 and 4 get crossed, thus changing their Chern numbers. The variation of Chern numbers produces the sign change in the transverse conductivity. Due to thermal fluctuations, the extremum of conductivity does not reach its quantized value of 2 (in units of e^2/h) but saturates at 1.8. The conductivity finally decreases down to zero when T reaches T_c, as it should.

It is also possible to choose the filling factors that place the Fermi level at zero temperature within a band. In these cases, there is no generic behavior, and the angle of the spin texture plays an important role. Some results are shown on Fig. 7 for the different filling factors $p=1/4$ [Fig. 7(c)] and $1/5$ [Fig. 7(d)].

Thus, these results show that in the mean field approximation a large variety of behaviors are possible in our model. The next step would be to study a model closer to the experimental situation of pyrochlores, where the variation of magnetic structure with temperature and applied field has been studied by neutron experiments,[15] allowing one to take into account the real crystallographic and magnetic structures of these systems.

ACKNOWLEDGMENTS

This work is partly supported by Université Joseph Fourier (Grenoble), by FCT Grant No. POCTI/FIS/58746/2004 (Portugal), and by the Polish State Committee for Scientific Research under PBZ/KBN Grants No. 044/P03/2001 and No. 2 P03B 053 25. V.D. thanks the Calouste Gulbenkian Foundation in Portugal for support.

[1] R. Karplus and J. M. Luttinger, Phys. Rev. **95**, 1154 (1954).
[2] L. Berger, Phys. Rev. B **2**, 4559 (1970).
[3] L. Berger, Phys. Rev. B **5**, 1862 (1972).
[4] J. Smit, Physica (Amsterdam) **21**, 877 (1954).
[5] J. Smit, Physica (Amsterdam) **24**, 39 (1958).
[6] P. Matl, N. P. Ong, Y. F. Yan, Y. Q. Li, D. Studebaker, T. Baum, and G. Doubinina, Phys. Rev. B **57**, 10248 (1998).
[7] J. Ye, Y. B. Kim, A. J. Millis, B. I. Shraiman, P. Majumdar, and Z. Tesanovic, Phys. Rev. Lett. **83**, 3737 (1999).
[8] S. H. Chun, M. B. Salamon, Y. Lyanda-Geller, P. M. Goldbart, and P. D. Han, Phys. Rev. Lett. **84**, 757 (2000).
[9] Gen Tatara and Hikaru Kawamura, J. Phys. Soc. Jpn. **71**, 2613 (2002).
[10] Hikaru Kawamura, Phys. Rev. Lett. **90**, 047202 (2003).
[11] P. Pureur, F. W. Fabris, J. Schaf, and I. A. Campbell, Europhys. Lett. **67**, 123 (2004).
[12] Toshifumi Taniguchi, Kensuke Yamanaka, Hideya Sumioka, Teruo Yamazaki, Yoshikazu Tabata, and Shuzo Kawarazaki, Phys. Rev. Lett. **93**, 246605 (2004).
[13] Y. Taguchi and Y. Tokura, Europhys. Lett. **54**, 401 (2001).
[14] Y. Taguchi, T. Sasaki, S. Awaji, Y. Iwasa, T. Tayama, T. Sakakibara, S. Iguchi, T. Ito, and Y. Tokura, Phys. Rev. Lett. **90**, 257202 (2003).
[15] Yukio Yasui, Satoshi Iikubo, Hiroshi Harashina, Taketomo Kageyama, Masafumi Ito, Masatoshi Sato, and Kazuhisa Kakurai, J. Phys. Soc. Jpn. **72**, 865 (2003).
[16] K. Ohgushi, S. Murakami, and N. Nagaosa, Phys. Rev. B **62**, R6065 (2000).
[17] Shigeki Onoda and Naoto Nagaosa, Phys. Rev. Lett. **90**, 196602 (2003).
[18] Taketomo Kageyama, S. Iikubo, S. Yoshii, Y. Kondo, M. Sato, and Y. Iye, J. Phys. Soc. Jpn. **70**, 3006 (2001).
[19] T. Katsufuji, H. Y. Hwang, and S.-W. Cheong, Phys. Rev. Lett. **84**, 1998 (2000).
[20] S. Yoshii, S. Iikubo, T. Kageyama, K. Oda, Y. Kondo, K. Murata, and M. Sato, J. Phys. Soc. Jpn. **69**, 3777 (2000).
[21] M. Elhajal, B. Canals, and C. Lacroix, Phys. Rev. B **66**, 014422 (2002).
[22] Masaru Onoda and Naoto Nagaosa, J. Phys. Soc. Jpn. **71**, 19 (2002).
[23] D. J. Thouless, M. Kohmoto, M. P. Nightingale, and M. den Nijs, Phys. Rev. Lett. **49**, 405 (1982).
[24] D. J. Thouless, Phys. Rev. B **27**, 6083 (1983).
[25] J. E. Avron, R. Seiler, and B. Simon, Phys. Rev. Lett. **51**, 51 (1983).
[26] F. D. M Haldane, Phys. Rev. Lett. **93**, 206602 (2004).
[27] A. Mielke, J. Phys. A **24**, L73 (1991).